# *Ab initio* block-Lanczos calculation of the Auger spectra of $SiF_4$: Strong two-hole localization effects and foreign imaging

F. O. Gottfried and L. S. Cederbaum
*Theoretische Chemie, Physikalisch-Chemisches Institut, Universität Heidelberg, 69120 Heidelberg, Germany*

F. Tarantelli
*Dipartimento di Chimica, Universitàa di Perugia, I-06123 Perugia, Italy*
(Received 30 May 1995)

The outer valence double-ionization spectrum of $SiF_4$ is investigated by performing accurate *ab initio* Green's-function calculations based on a newly implemented block-Lanczos algorithm. An analysis of the double-hole density in the correlated states of $SiF_4^{2+}$ proves that pronounced hole-localization phenomena at the fluorine atoms take place in all the final dicationic states of the Auger decay. We discuss how these phenomena are at the origin of the observed fluorine and silicon Auger spectral profiles and, in particular, how they provide a complete and conclusive account of *all* the peaks appearing in the Si $LVV$ spectrum. Confirming this, a simple convolution of appropriate intra-atomic components of the computed two-hole density distribution is shown to reproduce the measured spectra in every detail. The recently introduced *foreign-imaging* phenomenon is fully confirmed by the present extended calculations.

PACS number(s): 33.20.−t, 31.15.Ar, 32.80.Hd

## I. INTRODUCTION

Since the first results on the Auger spectra of silicon tetrafluoride were published by Rye and Houston [1], their interpretation, especially of the silicon spectrum, is still subject to controversial discussions. The spectra were first reported using electron impact ionization [1] and have later been confirmed using synchrotron radiation [2–4]. The Si ($LVV$) spectrum is at the center of interest because of its unusual spectral profile consisting of six broad bands where, according to an atomic self-imaging picture of molecular Auger spectroscopy, only three separated regions were expected. Rye and Houston explained this apparent ''doubling'' by postulating that the two valence holes in a single configuration final state appear spatially in the same Si–F bond or in different bonds. They supported their interpretation by doing calculations based on a semiempirical model and on several assumptions. The most important is the use of only two hole-hole interaction values (often referred to as $U$), one for localization in one Si–F bond and another for delocalization involving two Si–F bonds. This description was used by Aksela *et al.* [2] but with a larger set of $U$ values in order to account for the different Auger lines. Ferrett *et al.* [3] offered a different approach based on a pure molecular orbital picture. They described the final states with simple two-hole configurations but no explicit spectral assignment could be given. de Souza, Morin, and Nenner [4], refined that model but already pointed out that it might be neccessary to go beyond these simple models and take final-state configuration interaction into account.

Recently, Tarantelli and Cederbaum [5] carried out a preliminary study of the silicon spectrum of $SiF_4$ with a simplified Green's function method accounting for configuration interaction in the final diagram state space and a model estimate of relaxation effects. Despite not being able to diagonalize the full matrices, these restricted calculations including only the $2h$ configuration space clearly suggested the occurrence of pronounced hole localization at the fluorine atoms in all the 107 final diagram states, with very little and uniform hole density at the silicon. Guided by this finding, the authors proposed a general model, referred to as *foreign imaging*, capable of fully explaining the central atom Auger spectrum of $SiF_4$ and similar systems. The conclusions of that work have subsequently received some further indirect support by semiempirical symmetry restricted independent-particle calculations of Larkins, McColl, and Chelkowska [6], which, not describing hole-localization effects [7–9], could account only for four of the six peaks observed: such failure of the independent-particle model can indeed be precisely anticipated [5] once the occurrence of hole-localization phenomena is ascertained. Larkins, McColl, and Chelkowska proposed instead [6] that the missing peaks be attributed to unaccounted final-state correlation satellites.

The full *ab initio* calculation including electron correlation effects of the whole double ionization spectrum of $SiF_4$ is needed to conclusively settle the question of its interpretation and, which is of vast consequences in Auger spectroscopy, of the existence of the *foreign-imaging* phenomenon. Such calculation, until now beyond the reach of the current computational technologies, has become feasible by employing a block-Lanczos method, which, in our case, ensures fast convergence on the envelope of the energy distribution of the two-hole pole strength of the Green's function. In this paper we present the results of these calculations. With the knowledge of the correlated *ab initio* wave functions and energies of the dicationic states we have investigated the extent to which hole localization takes place and how it affects the energy position and appearance of the Auger peaks.

## II. COMPUTATIONAL DETAILS

Many dicationic states of the outer valence part of the double-ionization spectrum of $SiF_4$ were computed. This

 

was done within a theoretical framework based on two-particle Green's functions. The second-order approximation scheme used for the two-particle propagator is known as the algebraic diagrammatic construction (ADC) and has already been discussed extensively in the literature [13–18]. For a general overview of the theory and its application to Auger spectroscopy see Ref. [19]. We would like to mention that other computational approaches to Auger spectra are available in the literature. An incomplete list comprises Refs. [20,21]. We briefly recall here that the ADC formulation of the spectral representation of the propagator leads, at any given order of perturbation theory (as defined with respect to the neutral ground-state Fock operator), to a symmetric eigenvalue problem in the space of the dicationic configurations of the system under study. The double-ionization energies appear as eigenvalues and the eigenvectors are related to the residue amplitudes of the propagator. In the second-order scheme, ADC(2), the configuration space comprises all the two-hole ($2h$) configurations and all their single exitations ($3h1p$), defined in the basis of the neutral ground-state Hartree-Fock orbitals. The resulting eigenvalues give size-consistent ionization energies that are correct beyond second order for main states (i.e., states perturbatively derived from $2h$ space) and beyond first order for satellite states (derived from $3h1p$ configurations).

The calculations of the present work have been carried out in a triple-zeta basis set [22,23] including polarization functions [24]. The experimental Si–F bond length of 1.56 Å [25] has been used. The active molecular orbital space in $T_d$ symmetry in the ADC calculations comprises 97 Hartree-Fock orbitals (20 occupied). The ADC matrices range in size from 51 255 to 73 200, depending on space-spin symmetry (in the $D_2$ subgroup).

Using ADC(2) we computed double-ionization potentials (DIP's) and pole strength distribution of the outer valence dicationic states of $SiF_4$ in the energy range extending up to 120 eV. It is expected that the number of dicationic states characterized by a significant $2h$ projection, and thus relevant to the description of the Auger spectra, is of the order of $10^3$, with an average density well exceeding 10 states/eV. To selectively extract these many exact roots of large eigenvalue equations is of course very problematic. On the other hand, exactly because of the high density of relevant states, rather than in individual eigenvectors, we are interested in computing with enough accuracy the *envelope* of the dense pole strength distribution which, as will be discussed, can be related to the Auger spectrum. This task can be accomplished very effectively by employing a block-Lanczos procedure using as seed the $2h$ configuration space (main space). The ordinary, simple-vector, Lanczos algorithm was previously used, in connection with Auger spectroscopy, to extract selected roots in configuration calculations [10–12]. The block-Lanczos technique we use here can be shown [26,27] to provide a convergence rate on the ''spectrum'' of main space components, which is exponential in the width of the lines making up the spectrum. The fact that the block-Lanczos method provides the moments of the spectrum with respect to its starting space (all $2h$ components) with a high uniform accuracy, as well as its enhanced convergence properties make this approach decisively superior to the ordinary Lanczos algorithm. In the present case, with an assumed width of $\sim$ 1.5 eV, full convergence on the whole spectrum was obtained after 100 block-Lanczos iterations. The states up to about 60 eV were also *individually* converged.

TABLE I. Mulliken population analysis of the molecular orbitals of the valence shell (divided into inner and outer valence shell) of $SiF_4$.

| State | HF energy (eV) | Si | SiF | F | FF |
|---|---|---|---|---|---|
| $2a_1$ | -45.8086 | 0.0264 | 0.1262 | 0.8353 | 0.0060 |
| $2t_2$ | -44.7362 | 0.0140 | 0.1139 | 0.8752 | -0.0016 |
| $3a_1$ | -23.6242 | 0.1165 | 0.1383 | 0.7231 | 0.0111 |
| $3t_2$ | -21.4722 | 0.0795 | 0.1196 | 0.7875 | 0.0067 |
| $1e$ | -20.0131 | 0.0120 | 0.0810 | 0.8882 | 0.0094 |
| $4t_2$ | -19.4748 | 0.0172 | 0.0949 | 0.9061 | -0.0091 |
| $1t_1$ | -18.5263 | 0.0000 | 0.0000 | 1.0460 | -0.0230 |

## III. DICATIONIC STATES AND DOUBLE-IONIZATION ENERGIES

For an ionic molecule like $SiF_4$ one expects that the outer valence electron density is mainly located on the electronegative constituent. In the neutral ground state the electronic structure of the system can adequately be described by a valence bond model with an ionic $\sigma$ bond between the silicon and each flourine atom (where the electrons are strongly displaced towards the fluorines) and three nonbonding, nonoverlapping, electron distributions (lone pairs) concentrated around each fluorine. The electronic Hartree-Fock $T_d$ ground-state configuration of $SiF_4$ is

$$(\text{core})(2a_1)^2(2t_2)^6(3a_1)^2(3t_2)^6(1e)^4(4t_2)^6(1t_1)^6. \quad (1)$$

An interpretation of the molecular orbitals can be obtained by performing a Mulliken population analysis (see Table I). The $K$ and $L$ shells of the silicon atom as well as the $K$ shell of the fluorine atoms were considered as core. The $L$ shell of the silicon consists of the two states $1a_2$ and $1t_2$, which are the Si $2s$ and $2p$ orbitals, respectively. The next seven orbitals build up the valence shell. It can be subdivided into two regions: the inner valence part (orbitals $2a_1$ and $2t_2$) and the outer valence part. The orbitals of the inner valence shell are mainly of fluorine $2s$ character. The bonding is exercised mostly through the $3a_1$ and $3t_2$ orbitals of the outer valence part. The three outermost orbitals represent the fluorine lone pairs.

The double-ionization energies and $2h$ composition of the most important exactly computed states are reported in Table II. According to the character of the molecular orbitals, one expects the following distribution of the outer valence two-hole states with increasing energy: (fluorine lone pair)$^{-2}$, (fluorine lone pair)$^{-1}$ ($\sigma$ bond)$^{-1}$ and ($\sigma$ bond)$^{-2}$. These three regions can easily be identified in Table II in the energy region from 37 up to 47 eV. The singlet–triplet splitting within this part of the spectrum is of the order of several $10^{-1}$ eV. In the energy region ranging from 48 up to 57 eV this same structure is repeated twice, once for the lower-lying triplet states and once for the singlet states, with a singlet-triplet splitting here of the order of several eV. This

TABLE II. Computed double-ionization potential (DIP) and composition of the outer valence dicationic states of $SiF_4$ up to 60 eV (converged at least to $10^{-8}$ eV). The composition reported is given by the square of the $2h$ components of the ADC eigenvectors with a pole strength (PS) larger than 0.01. The $2h$ configurations are indicated by the occupied orbitals of $SiF_4$ from which the two electrons are removed. States with a PS component larger than 0.1 are boldfaced.

| State | DIP (eV) | PS | $2h$ composition |
|---|---|---|---|
| $^3T_1$ | **37.5190** | 0.856 | $0.694(1t_1)$ $0.076(1e1t_1)$ $0.059(4t_21t_1)$ $0.012(4t_2)$ $0.008(1e4t_2)$ $0.003(3t_21t_1)$ $0.002(3t_21e)$ $0.001(3t_24t_2)$ |
| $^1E$ | **37.5296** | 0.857 | $0.678(1t_1)$ $0.130(4t_21t_1)$ $0.022(4t_2)$ $0.015(3t_21t_1)$ $0.010(1e)0.001(3t_24t_2)$ |
| $^1T_2$ | **37.9480** | 0.856 | $0.539(1t_1)$ $0.126(4t_21t_1)$ $0.088(1e1t_1)$ $0.076(1e4t_2)$ $0.014(3t_21t_1)$ $0.007(4t_2)$ $0.003(3t_24t_2)$ $0.003(3t_21e)$ |
| $^1A_2$ | **38.2884** | 0.857 | $0.857(4t_21t_1)$ |
| $^1A_1$ | **38.4219** | 0.857 | $0.552(1t_1)$ $0.174(4t_2)$ $0.092(1e)$ $0.038(3t_24t_2)$ |
| $^3T_1$ | **38.5110** | 0.857 | $0.644(4t_21t_1)$ $0.161(1e1t_1)$ $0.027(1e4t_2)$ $0.010(4t_2)$ $0.009(1t_1)0.002(3a_11t_1)$ $0.002(3t_24t_2)$ |
| $^1T_1$ | **38.6172** | 0.855 | $0.466(1e1t_1)$ $0.375(4t_21t_1)$ $0.007(3t_24t_2)$ $0.003(3t_21e)$ $0.002(3a_11t_1)0.001(1e4t_2)$ |
| $^3T_2$ | **38.6352** | 0.855 | $0.682(4t_21t_1)$ $0.073(1e1t_1)$ $0.048(3t_21t_1)$ $0.036(1e4t_2)$ $0.007(3t_24t_2)0.006(3t_21e)$ $0.002(3a_14t_2)$ |
| $^3E$ | **38.6842** | 0.856 | $0.761(4t_21t_1)$ $0.059(3t_21t_1)$ $0.033(3t_24t_2)$ $0.003(3a_11e)$ |
| $^3T_2$ | **38.8254** | 0.855 | $0.779(1e1t_1)$ $0.065(4t_21t_1)$ $0.006(1e4t_2)$ $0.002(3t_24t_2)$ $0.001(3t_21t_1)$ |
| $^1T_2$ | **39.0215** | 0.855 | $0.233(1e1t_1)$ $0.220(4t_2)$ $0.209(4t_21t_1)$ $0.079(1e4t_2)$ $0.066(1t_1)$ $0.019(3t_21e)$ $0.015(3t_24t_2)$ $0.009(3t_21t_1)$ $0.003(3a_14t_2)$ $0.001(3t_2)$ |
| $^3A_2$ | **39.2435** | 0.854 | $0.523(4t_21t_1)$ $0.169(1e)$ $0.160(3t_21t_1)$ $0.001(2t_21t_1)$ |
| $^3T_1$ | **39.2662** | 0.854 | $0.336(1e1t_1)$ $0.267(1e4t_2)$ $0.172(4t_2)$ $0.045(4t_21t_1)$ $0.019(1t_1)$ $0.010(3t_24t_2)$ $0.001(3t_2)$ $0.001(3a_11t_1)$ |
| $^1E$ | **39.5472** | 0.852 | $0.355(1e)$ $0.284(4t_21t_1)$ $0.133(4t_2)$ $0.041(1t_1)$ $0.022(3t_24t_2)$ $0.010(3t_21t_1)$ $0.004(3t_2)$ $0.001(3a_11e)$ |
| $^1T_1$ | **39.7407** | 0.852 | $0.407(1e4t_2)$ $0.168(4t_21t_1)$ $0.144(1e1t_1)$ $0.057(3t_24t_2)$ $0.046(3t_21e)0.019(3t_21t_1)$ $0.009(3a_11t_1)$ |
| $^1E$ | **39.8174** | 0.856 | $0.447(4t_2)$ $0.273(3t_21t_1)$ $0.071(4t_21t_1)$ $0.042(1e)$ $0.011(3t_24t_2)$ $0.007(3t_2)$ $0.002(3a_11e)$ $0.002(1t_1)$ |
| $^1T_2$ | **39.9234** | 0.855 | $0.318(4t_2)$ $0.201(3t_21t_1)$ $0.176(1e4t_2)$ $0.072(4t_21t_1)$ $0.036(3t_21e)$ $0.036(3t_24t_2)$ $0.007(1e1t_1)$ $0.006(1t_1)$ $0.002(3a_13t_2)$ |
| $^1A_1$ | **39.9726** | 0.851 | $0.435(1e)$ $0.365(4t_2)$ $0.028(3t_24t_2)$ $0.012(1t_1)$ $0.010(3t_2)$ |
| $^3T_2$ | **39.9902** | 0.852 | $0.703(1e4t_2)$ $0.119(3t_21t_1)$ $0.011(3t_21e)$ $0.010(3t_24t_2)$ $0.008(4t_21t_1)$ |
| $^3T_1$ | **40.0222** | 0.855 | $0.383(4t_2)$ $0.320(3t_21t_1)$ $0.054(1e4t_2)$ $0.048(1e1t_1)$ $0.036(3t_21e)0.006(1t_1)$ $0.004(3a_11t_1)$ $0.002(3t_2)$ |
| $^1T_1$ | **40.1552** | 0.855 | $0.562(3t_21t_1)$ $0.207(1e4t_2)$ $0.035(4t_21t_1)$ $0.033(1e1t_1)$ $0.009(3t_21e)0.004(3a_11t_1)$ $0.003(3t_24t_2)$ |
| $^3A_2$ | **40.2965** | 0.853 | $0.430(1e)$ $0.423(3t_21t_1)$ |
| $^1A_2$ | **40.4230** | 0.854 | $0.852(3t_21t_1)$ $0.002(2t_21t_1)$ |
| $^1T_2$ | **40.6161** | 0.853 | $0.246(3t_21e)$ $0.245(3t_21t_1)$ $0.168(4t_21t_1)$ $0.063(1e4t_2)$ $0.047(1e1t_1)$ $0.039(3t_24t_2)$ $0.014(1t_1)$ $0.011(3a_14t_2)$ $0.010(4t_2)$ $0.006(3t_2)0.001(3a_13t_2)$ |
| $^3T_1$ | **40.7991** | 0.853 | $0.322(3t_21t_1)$ $0.177(1e4t_2)$ $0.102(3t_24t_2)$ $0.080(3t_21e)$ $0.076(4t_2)$ |

TABLE II. (*Continued.*)

| State | DIP (eV) | PS | $2h$ composition |
|---|---|---|---|
| | | | $0.049(3a_1 1t_1)$ $0.025(3t_2)$ $0.015(4t_2 1t_1)$ $0.005(1e 1t_1)$ |
| $^3E$ | **40.8570** | 0.854 | $0.576(3t_2 1t_1)$ $0.258(3t_2 4t_2)$ $0.010(4t_2 1t_1)$ $0.008(3a_1 1e)$ |
| $^1E$ | **40.9797** | 0.854 | $0.455(3t_2 4t_2)$ $0.197(1e)$ $0.074(4t_2 1t_1)$ $0.073(3t_2 1t_1)$ $0.028(3t_2)$ $0.010(4t_2)$ $0.008(3a_1 1e)$ $0.008(1t_1)$ |
| $^3T_2$ | **41.0332** | 0.853 | $0.454(3t_2 1t_1)$ $0.245(3t_2 4t_2)$ $0.094(3t_2 1e)$ $0.027(1e 4t_2)$ $0.016(3a_1 4t_2)$ $0.014(4t_2 1t_1)$ |
| $^3T_1$ | **41.1683** | 0.852 | $0.438(3t_2 4t_2)$ $0.124(3t_2 1e)$ $0.108(3t_2 1t_1)$ $0.074(1e 4t_2)$ $0.036(4t_2)$ $0.033(1e 1t_1)$ $0.013(1t_1)$ $0.011(3a_1 1t_1)$ $0.007(4t_2 1t_1)$ $0.004(3t_2)$ |
| $^3A_1$ | **41.5131** | 0.854 | $0.852(3t_2 4t_2)$ $0.001(2t_2 3t_2)$ |
| $^1T_2$ | **41.5404** | 0.853 | $0.302(3t_2 4t_2)$ $0.113(3t_2)$ $0.101(3t_2 1e)$ $0.089(1e 4t_2)$ $0.086(4t_2)$ $0.075(1e 1t_1)$ $0.045(3a_1 4t_2)$ $0.021(1t_1)$ $0.008(4t_2 1t_1)$ $0.007(3a_1 3t_2)$ $0.004(3t_2 1t_1)$ $0.001(2t_2 4t_2)$ |
| $^1T_1$ | **41.5985** | 0.852 | $0.457(3t_2 1e)$ $0.323(3t_2 4t_2)$ $0.031(3t_2 1t_1)$ $0.015(4t_2 1t_1)$ $0.014(1e 4t_2)$ $0.011(1e 1t_1)$ |
| $^3T_2$ | **41.6977** | 0.852 | $0.436(3t_2 1e)$ $0.392(3t_2 4t_2)$ $0.018(3t_2 1t_1)$ $0.002(4t_2 1t_1)$ $0.002(1e 4t_2)$ |
| $^3T_1$ | **42.0327** | 0.852 | $0.337(3t_2 1e)$ $0.291(3a_1 1t_1)$ $0.123(3t_2 4t_2)$ $0.044(1e 4t_2)$ $0.034(3t_2)$ $0.007(4t_2 1t_1)$ $0.007(1e 1t_1)$ $0.004(4t_2)$ $0.003(1t_1)$ |
| $^1A_1$ | **42.1072** | 0.855 | $0.346(3t_2)$ $0.260(3t_2 4t_2)$ $0.119(4t_2)$ $0.094(1e)$ $0.030(1t_1)$ $0.003(3a_1)$ $0.002(2t_2 4t_2)$ |
| $^1E$ | **42.1893** | 0.851 | $0.246(3t_2 4t_2)$ $0.177(3t_2)$ $0.167(3t_2 1t_1)$ $0.140(3a_1 1e)$ $0.061(4t_2)$ $0.051(4t_2 1t_1)$ $0.005(1e)$ $0.002(2t_2 3t_2)$ $0.001(2t_2 4t_2)$ |
| $^1T_1$ | **42.3228** | 0.853 | $0.590(3a_1 1t_1)$ $0.150(3t_2 4t_2)$ $0.086(3t_2 1e)$ $0.016(1e 4t_2)$ $0.008(3t_2 1t_1)$ $0.001(2t_2 4t_2)$ $0.001(1e 1t_1)$ |
| $^3T_2$ | **43.1390** | 0.851 | $0.498(3a_1 4t_2)$ $0.150(3t_2 1e)$ $0.095(3t_2 4t_2)$ $0.043(3t_2 1t_1)$ $0.029(3a_1 3t_2)$ $0.019(1e 4t_2)$ $0.014(4t_2 1t_1)$ $0.001(2a_1 4t_2)$ |
| $^3E$ | **43.1651** | 0.848 | $0.491(3a_1 1e)$ $0.275(3t_2 4t_2)$ $0.061(3t_2 1t_1)$ $0.018(4t_2 1t_1)$ $0.001(2a_1 1e)$ |
| $^3T_1$ | **43.2020** | 0.851 | $0.520(3t_2)$ $0.246(3a_1 1t_1)$ $0.055(3t_2 4t_2)$ $0.012(1e 4t_2)$ $0.006(1e 1t_1)$ $0.004(4t_2 1t_1)$ $0.003(1t_1)$ $0.003(2t_2 3t_2)$ |
| $^1T_2$ | **43.3452** | 0.851 | $0.460(3a_1 4t_2)$ $0.238(3t_2)$ $0.052(3t_2 1e)$ $0.032(3t_2 1t_1)$ $0.028(3a_1 3t_2)$ $0.019(4t_2)$ $0.009(1e 4t_2)$ $0.006(1e 1t_1)$ $0.002(4t_2 1t_1)$ $0.001(3t_2 4t_2)$ |
| $^1E$ | **43.7202** | 0.850 | $0.414(3t_2)$ $0.402(3a_1 1e)$ $0.013(3t_2 1t_1)$ $0.009(4t_2)$ $0.004(1e)$ $0.004(3t_2 4t_2)$ $0.001(2t_2 3t_2)$ $0.001(1t_1)$ |
| $^1T_2$ | **44.0391** | 0.853 | $0.336(3a_1 3t_2)$ $0.196(3t_2)$ $0.142(3t_2 4t_2)$ $0.053(3t_2 1e)$ $0.051(3t_2 1t_1)$ $0.027(1e 4t_2)$ $0.027(4t_2)$ $0.015(4t_2 1t_1)$ $0.001(3a_1 4t_2)$ $0.001(2t_2 3t_2)$ $0.001(1e 1t_1)$ $0.001(1t_1)$ |
| $^3T_2$ | **45.2918** | 0.848 | $0.622(3a_1 3t_2)$ $0.154(3a_1 4t_2)$ $0.024(3t_2 1e)$ $0.021(3t_2 1t_1)$ $0.009(3t_2 4t_2)$ $0.007(4t_2 1t_1)$ $0.007(1e 4t_2)$ $0.002(2t_2 3a_1)$ $0.001(2a_1 3t_2)$ |
| $^1A_1$ | **46.3929** | 0.851 | $0.476(3a_1)$ $0.200(3t_2)$ $0.152(3t_2 4t_2)$ $0.016(4t_2)$ $0.002(2a_1 3a_1)$ $0.001(2t_2 3t_2)$ $0.001(1e)$ |
| $^3A_2$ | **48.3777** | 0.797 | $0.304(4t_2 1t_1)$ $0.255(3t_2 1t_1)$ $0.238(1e)$ |
| $^3T_1$ | **48.5056** | 0.798 | $0.167(1e 1t_1)$ $0.129(3t_2 1e)$ $0.120(1e 4t_2)$ $0.097(1t_1)$ $0.092(3t_2 4t_2)$ $0.061(4t_2)$ $0.045(4t_2 1t_1)$ $0.044(3t_2 1t_1)$ $0.042(3t_2)$ |

TABLE II. (*Continued.*)

| State | DIP (eV) | PS | 2*h* composition |
|---|---|---|---|
| $^3T_1$ | **50.3013** | 0.797 | 0.231($3a_1 1t_1$) 0.206($3t_2$) 0.126($3t_2 1e$) 0.087($4t_2$) 0.055($1e 4t_2$) 0.047($3t_2 1t_1$) 0.022($3t_2 4t_2$) 0.022($4t_2 1t_1$) 0.001($2a_1 1t_1$) |
| $^3E$ | **50.3875** | 0.798 | 0.329($3a_1 1e$) 0.266($3t_2 4t_2$) 0.142($3t_2 1t_1$) 0.059($4t_2 1t_1$) 0.001($2a_1 1e$) |
| $^3T_2$ | **50.4999** | 0.799 | 0.185($3a_1 3t_2$) 0.168($3a_1 4t_2$) 0.135($3t_2 1t_1$) 0.120($3t_2 1e$) 0.085($3t_2 4t_2$) 0.056($4t_2 1t_1$) 0.048($1e 4t_2$) |
| $^1T_1$ | **51.0360** | 0.800 | 0.216($4t_2 1t_1$) 0.185($1e 1t_1$) 0.165($3t_2 1t_1$) 0.137($1e 4t_2$) 0.097($3t_2 1e$) |
| $^1E$ | **51.0880** | 0.801 | 0.223($1e$) 0.150($4t_2 1t_1$) 0.133($3t_2 1t_1$) 0.116($1t_1$) 0.083($3t_2 4t_2$)0.066($4t_2$) 0.029($3t_2$) |
| $^1T_2$ | **51.1347** | 0.801 | 0.188($1e 1t_1$) 0.148($1t_1$) 0.121($1e 4t_2$) 0.120($3t_2 4t_2$) 0.099($3t_2 1e$)0.078($4t_2$) 0.046($3t_2$) |
| $^1T_2$ | **52.3675** | 0.800 | 0.155($1e 1t_1$) 0.136($4t_2 1t_1$) 0.124($1e 4t_2$) 0.112($3t_2 1t_1$) 0.077($3t_2 1e$) 0.051($3a_1 3t_2$) 0.048($3t_2$) 0.038($1t_1$) 0.036($4t_2$) 0.013($3a_1 4t_2$) 0.003($2t_2$) 0.003($2a_1 2t_2$) 0.001($2t_2 4t_2$) |
| $^1A_1$ | **52.4680** | 0.803 | 0.277($3t_2 4t_2$) 0.205($1t_1$) 0.186($1e$) 0.060($4t_2$) 0.060($3a_1$) 0.005($3t_2$) 0.005($2t_2$) 0.002($2a_1 3a_1$) 0.001($2a_1$) |
| $^1T_1$ | **52.8853** | 0.794 | 0.290($3t_2 4t_2$) 0.228($3a_1 1t_1$) 0.137($3t_2 1e$) 0.057($1e 4t_2$) 0.053($3t_2 1t_1$)0.028($4t_2 1t_1$) 0.001($2t_2 1t_1$) |
| $^1E$ | **52.9610** | 0.012 | 0.004($3a_1 1e$) 0.003($3t_2$) 0.002($4t_2 1t_1$) 0.002($4t_2$) |
| $^1E$ | **53.0932** | 0.787 | 0.269($3a_1 1e$) 0.171($3t_2$) 0.147($3t_2 1t_1$) 0.094($4t_2$) 0.076($4t_2 1t_1$) 0.023($3t_2 4t_2$) 0.004($2t_2 1t_1$) 0.001($2t_2 4t_2$) 0.001($2a_1 1e$) |
| $^1T_2$ | **53.1052** | 0.797 | 0.185($3a_1 4t_2$) 0.148($3t_2 1t_1$) 0.127($3t_2 1e$) 0.098($3a_1 3t_2$) 0.076($3t_2$) 0.075($4t_2 1t_1$) 0.054($1e 4t_2$) 0.025($4t_2$) 0.003($2t_2 1t_1$) 0.003($3t_2 4t_2$) 0.001($2a_1 3t_2$) |
| $^1T_2$ | **56.1762** | 0.154 | 0.056($3a_1 3t_2$) 0.036($3t_2 4t_2$) 0.021($3a_1 4t_2$) 0.015($3t_2$) 0.005($4t_2 1t_1$) 0.005($4t_2$) 0.003($3t_2 1t_1$) 0.003($3t_2 1e$) 0.003($1e 4t_2$) 0.003($1e 1t_1$) 0.002($2t_2$) 0.001($2a_1 2t_2$) 0.001($2t_2 3t_2$) |
| $^1T_2$ | **56.2726** | 0.577 | 0.207($3a_1 3t_2$) 0.120($3t_2 4t_2$) 0.078($3a_1 4t_2$) 0.077($3t_2$) 0.018($1e 1t_1$) 0.015($4t_2 1t_1$) 0.012($4t_2$) 0.011($1e 4t_2$) 0.009($3t_2 1e$) 0.006($2t_2$) 0.006($3t_2 1t_1$) 0.005($2a_1 2t_2$) 0.005($1t_1$) 0.003($2t_2 3t_2$) 0.002($2t_2 3a_1$)0.001($2t_2 4t_2$) |
| $^1T_2$ | **56.3719** | 0.050 | 0.015($3a_1 3t_2$) 0.010($3t_2 4t_2$)0.009($3t_2$) 0.007($3a_1 4t_2$) 0.002($1e 1t_1$)0.002($4t_2 1t_1$) 0.001($3t_2 1e$) |
| $^1T_2$ | **56.6016** | 0.013 | 0.004($3a_1 3t_2$) 0.003($3t_2$) 0.002($3t_2 4t_2$) 0.001($4t_2 1t_1$) |
| $^1A_1$ | **56.6823** | 0.778 | 0.270($3a_1$) 0.251($3t_2$) 0.102($4t_2$) 0.072($3t_2 4t_2$) 0.034($1t_1$) 0.022($1e$) 0.014($2t_2$) 0.005($2t_2 4t_2$) 0.004($2t_2 3t_2$) 0.003($2a_1$) |
| $^1A_1$ | **56.9149** | 0.025 | 0.008($3t_2$) 0.007($3a_1$) 0.005($1e$) 0.003($3t_2 4t_2$) |
| $^1A_1$ | **57.0620** | 0.012 | 0.005($3t_2$) 0.003($4t_2$) 0.002($3a_1$) |

already gives a first indication on the character of the states, namely, that the states rising from 37–47 eV are pure ''two-site'' states with the two holes localized in two different $\sigma$ bonds, and that the states ranging from 48 to 57 eV are ''one-site'' states where the two holes are localized in the same $\sigma$ bond. In the following section these arguments will be made more quantitative.

Another important result emerging from these data is that already at low double-ionization energies a very strong two-hole configuration mixing in the composition of the most states arises. These observations point very clearly to an intractability of the $SiF_4$ double-ionization spectrum within an independent-particle framework and are consistent with the requirements dictated by atomic localization of positive charges. This was illustrated in detail for the case of $BF_3$ [9].

## IV. ATOMIC LOCALIZATION OF THE TWO HOLES IN THE DICATIONIC STATES

We now come back to the question of if and to what extent a localization of the two valence holes in the final states of the Auger process takes place. As reviewed in the Introduction, this gave reason for controversial interpretations for over a decade. Having the correlated wave functions at hand, we can now study this question in detail.

In analogy to the Mulliken population analysis we use a *two-hole population analysis* of the dicationic states [9]. By this analysis, the contributions of the $2h$ part of the ADC eigenvectors to the total pole strengths are expressed in terms of the atomic orbital $2h$ functions. This provides a well-defined way to analyze the pole strength in terms of *localized* atomic contributions. The sum of the contributions of the atomic-orbital (AO) hole pairs $p$, $q$ to the total pole strength where both $p$ and $q$ refer to basis functions centered on a given atom $A$ is the ''one-site'' pole strength of that atom, and measures the extent to which the dicationic state can be described as having both holes localized on atom $A$. Similarly, the ''two-site'' character of a state for each pair of atoms $A$ and $B$, describing the localized component with one hole localized on $A$ and the other on $B$, is measured by the sum of terms where $p$ and $q$ refer to basis functions centered on $A$ and $B$, respectively. Thus the predominance of one of these contributions for a given state indicates that the two vacancies are strongly localized in space (either at the same or each at another atomic center, according to the dominating component). States for which more than one component is significantly present are characterized instead as having correspondingly delocalized holes.

In the case of $SiF_4$ we can thus separate the total $2h$ pole strength of the ADC states in contributions that we denote as $Si^{-2}$ (two holes on the silicon atom), $F^{-2}$ (two holes on the same fluorine atom), $F_1^{-1}F_2^{-1}$ (two holes on different fluorine atoms), and $Si^{-1}F^{-1}$ (one hole on the silicon and one on a fluorine atom). The relevant results for the outer valence dicationic states in the energy region up to 60 eV are reported in Table III. At higher energy, most ADC eigenvectors are not individually fully converged and so their individual population analysis is not meaningful. To validate the following discussion, however, we point out that the *total* $2h$ distribution (envelope) is fully converged over the whole spectrum, as are also its separate population components.

The results of the population analysis show without ambiguity that *all* dicationic states of $SiF_4$ are dominated either by the fluorine one-site ($F^{-2}$) or by the fluorine two-site ($F_1^{-1}F_2^{-1}$) character. This means that the two holes are always strongly localized in space: for any given state they are either localized on the same fluorine atom, or each on another fluorine atom. This pronounced localization of the electron vacancies at the fluorine sites obviously characterizes their energies via hole-hole repulsion and, according to their similar hole distribution, the states cluster in eight energy separated groups. This confirms in full the similar results obtained in Ref. [5].

The computed average populations (in percent of the total $2h$ pole strength) for the eight groups of states are reported in Table IV. Here and in the following the groups are denoted by labels A to F, in order of increasing double-ionization energy. The table also reports the details of the characterization of the states in terms of the $s$ and $p$ shells of fluorine involved in the ionization. The grouping of states is evidenced in Fig. 1, where we show a Gaussian convolution of the computed total $2h$ pole strength distribution and a histogram plot of the density of states. As the figure illustrates, the density of states is relatively low in the right-hand side of the spectrum up to $\sim$60 eV. Here the shape of the convolution is determined essentially by a relatively small number of states dominated by $2h$ components. At higher energies, a massive increase in the density is computed, and the $2h$ character is spread over many states. However, far from becoming uniformly distributed, states continue to occur in evident very dense clusters and the shape of the $2h$ envelope reflects this pattern precisely. The results of the population analysis are illustrated in Fig. 2, where we have reported analogous separate contributions of the $F^{-2}$ and $F_1^{-1}F_2^{-1}$ components to the total $2h$ pole strength. This makes evident the alternating and complete dominance of one or the other component. One can also note here the close coincidence between the sum of the fluorine contributions and the total $2h$ curve. The difference between the two is due essentially to the $Si^{-1}F^{-1}$ component since the $Si^{-2}$ terms are systematically orders of magnitude smaller.

With the aid of these illustrations we can now analyze in more detail the various groups of states and their origin. The first group (labeled A in Table IV and in the figures). ranging from 37 to 47 eV is dominated by the $F_1^{-1}F_2^{-1}$ population. These states are clearly characterized as fluorine $p^{-2}$ in character, and have holes localized on two distinct fluorine atoms. The charge separation minimizes the hole-hole repulsion so that this group is found at the low-ionization energy side of the spectrum (high kinetic energy of the Auger electrons). In group A, due to the relatively large distance between the two holes, singlet-triplet pairs of states lie close in energy, separated by only a few tenths of eV. Group A is followed by its one-side counterpart group B, comprising $p^{-2}$ states with two holes confined on the same fluorine atom according to the large $F^{-2}$ component. The highest-lying states of group A and the lowest-lying states of group B are clearly separated in energy by a gap of almost 2 eV, the peaks themselves are separated by more than 10 eV. The data show that the states of group B actually split into two distinct subgroups, $B_1$ and $B_2$. The lower-energy side of $B_1$ is made

TABLE III. DIP's and two-hole atomic population analysis of the Green's function $2h$ pole strengths for the outer valence dicationic states of $SiF_4$ up to 60 eV (converged at least to $10^{-8}$ eV). States with a total pole strength larger than 0.1 are boldfaced.

| State | DIP (eV) | Population $Si^{-2}$ | $F^{-2}$ | $Si^{-1}F^{-1}$ | $F_1^{-1}F_2^{-1}$ | Total |
|---|---|---|---|---|---|---|
| $^3T_1$ | **37.5190** | 0.0000 | 0.0030 | 0.0106 | 0.8426 | 0.8563 |
| $^1E$ | **37.5296** | 0.0001 | 0.0013 | 0.0130 | 0.8423 | 0.8566 |
| $^1T_2$ | **37.9480** | 0.0003 | 0.0025 | 0.0233 | 0.8298 | 0.8559 |
| $^1A_2$ | **38.2884** | 0.0000 | -0.0008 | 0.0550 | 0.8032 | 0.8574 |
| $^1A_1$ | **38.4219** | 0.0011 | 0.0036 | 0.0345 | 0.8175 | 0.8567 |
| $^3T_1$ | **38.5110** | 0.0002 | 0.0008 | 0.0546 | 0.8011 | 0.8567 |
| $^1T_1$ | **38.6172** | 0.0000 | 0.0003 | 0.0502 | 0.8045 | 0.8551 |
| $^3T_2$ | **38.6352** | 0.0003 | 0.0031 | 0.0565 | 0.7955 | 0.8555 |
| $^3E$ | **38.6842** | 0.0003 | 0.0041 | 0.0580 | 0.7937 | 0.8560 |
| $^3T_2$ | **38.8254** | 0.0000 | -0.0002 | 0.0465 | 0.8085 | 0.8548 |
| $^1T_2$ | **39.0215** | 0.0013 | 0.0025 | 0.0649 | 0.7860 | 0.8547 |
| $^3A_2$ | **39.2435** | 0.0005 | 0.0084 | 0.0765 | 0.7684 | 0.8538 |
| $^3T_1$ | **39.2662** | 0.0016 | 0.0030 | 0.0708 | 0.7782 | 0.8536 |
| $^1E$ | **39.5472** | 0.0018 | 0.0049 | 0.0773 | 0.7680 | 0.8520 |
| $^1T_1$ | **39.7407** | 0.0020 | 0.0037 | 0.0828 | 0.7635 | 0.8521 |
| $^1E$ | **39.8174** | 0.0020 | 0.0006 | 0.0982 | 0.7547 | 0.8555 |
| $^1T_2$ | **39.9234** | 0.0022 | 0.0008 | 0.0958 | 0.7559 | 0.8547 |
| $^1A_1$ | **39.9726** | 0.0029 | 0.0013 | 0.0912 | 0.7553 | 0.8507 |
| $^3T_2$ | **39.9902** | 0.0024 | 0.0003 | 0.0942 | 0.7555 | 0.8524 |
| $^3T_1$ | **40.0222** | 0.0020 | 0.0032 | 0.1025 | 0.7468 | 0.8546 |
| $^1T_1$ | **40.1552** | 0.0008 | 0.0006 | 0.1083 | 0.7450 | 0.8547 |
| $^3A_2$ | **40.2965** | 0.0012 | 0.0000 | 0.1002 | 0.7515 | 0.8529 |
| $^1A_2$ | **40.4230** | 0.0000 | -0.0013 | 0.1106 | 0.7445 | 0.8537 |
| $^1T_2$ | **40.6161** | 0.0026 | 0.0070 | 0.1120 | 0.7317 | 0.8533 |
| $^3T_1$ | **40.7991** | 0.0023 | 0.0077 | 0.1133 | 0.7295 | 0.8528 |
| $^3E$ | **40.8570** | 0.0021 | 0.0017 | 0.1252 | 0.7250 | 0.8540 |
| $^1E$ | **40.9797** | 0.0045 | 0.0040 | 0.1222 | 0.7229 | 0.8535 |
| $^3T_2$ | **41.0332** | 0.0029 | 0.0037 | 0.1273 | 0.7194 | 0.8533 |
| $^3T_1$ | **41.1683** | 0.0051 | 0.0079 | 0.1346 | 0.7049 | 0.8525 |
| $^3A_1$ | **41.5131** | 0.0071 | -0.0016 | 0.1533 | 0.6949 | 0.8536 |
| $^1T_2$ | **41.5404** | 0.0062 | 0.0111 | 0.1348 | 0.7009 | 0.8529 |
| $^1T_1$ | **41.5985** | 0.0060 | 0.0013 | 0.1441 | 0.7005 | 0.8519 |
| $^3T_2$ | **41.6977** | 0.0063 | 0.0003 | 0.1477 | 0.6978 | 0.8521 |
| $^3T_1$ | **42.0327** | 0.0047 | 0.0068 | 0.1492 | 0.6917 | 0.8524 |
| $^1A_1$ | **42.1072** | 0.0082 | 0.0071 | 0.1468 | 0.6925 | 0.8545 |
| $^1E$ | **42.1893** | 0.0076 | 0.0133 | 0.1555 | 0.6742 | 0.8506 |
| $^1T_1$ | **42.3228** | 0.0018 | 0.0019 | 0.1467 | 0.7025 | 0.8529 |
| $^3T_2$ | **43.1390** | 0.0076 | 0.0151 | 0.1650 | 0.6630 | 0.8507 |
| $^3E$ | **43.1651** | 0.0067 | 0.0216 | 0.1606 | 0.6591 | 0.8481 |
| $^3T_1$ | **43.2020** | 0.0099 | 0.0071 | 0.1767 | 0.6571 | 0.8508 |
| $^1T_2$ | **43.3452** | 0.0099 | 0.0060 | 0.1770 | 0.6576 | 0.8505 |
| $^1E$ | **43.7202** | 0.0111 | 0.0032 | 0.1837 | 0.6521 | 0.8501 |
| $^1T_2$ | **44.0391** | 0.0136 | 0.0209 | 0.1866 | 0.6323 | 0.8533 |
| $^3T_2$ | **45.2918** | 0.0171 | 0.0206 | 0.2091 | 0.6012 | 0.8479 |
| $^1A_1$ | **46.3929** | 0.0195 | 0.0346 | 0.2158 | 0.5811 | 0.8510 |
| $^3A_2$ | **48.3777** | 0.0007 | 0.7231 | 0.0694 | 0.0041 | 0.7972 |
| $^3T_1$ | **48.5056** | 0.0024 | 0.7071 | 0.0779 | 0.0106 | 0.7981 |
| $^3T_1$ | **50.3013** | 0.0053 | 0.6368 | 0.1410 | 0.0142 | 0.7973 |
| $^3E$ | **50.3875** | 0.0052 | 0.6275 | 0.1430 | 0.0222 | 0.7979 |
| $^3T_2$ | **50.4999** | 0.0071 | 0.6114 | 0.1499 | 0.0304 | 0.7989 |
| $^1T_1$ | **51.0360** | 0.0010 | 0.7288 | 0.0691 | 0.0012 | 0.8001 |
| $^1E$ | **51.0880** | 0.0017 | 0.7258 | 0.0712 | 0.0021 | 0.8008 |
| $^1T_2$ | **51.1347** | 0.0025 | 0.7224 | 0.0733 | 0.0032 | 0.8014 |

TABLE III. (*Continued.*)

| State | DIP (eV) | Population $Si^{-2}$ | $F^{-2}$ | $Si^{-1}F^{-1}$ | $F_1^{-1}F_2^{-1}$ | Total |
|---|---|---|---|---|---|---|
| $^1T_2$ | **52.3675** | 0.0038 | 0.7082 | 0.0823 | 0.0058 | 0.8002 |
| $^1A_1$ | **52.4680** | 0.0050 | 0.7031 | 0.0883 | 0.0065 | 0.8029 |
| $^1T_1$ | **52.8853** | 0.0041 | 0.6417 | 0.1436 | 0.0050 | 0.7943 |
| $^1E$ | **52.9610** | 0.0001 | 0.0096 | 0.0022 | 0.0004 | 0.0123 |
| $^1E$ | **53.0932** | 0.0058 | 0.6151 | 0.1463 | 0.0200 | 0.7872 |
| $^1T_2$ | **53.1052** | 0.0063 | 0.6217 | 0.1500 | 0.0187 | 0.7967 |
| $^1T_2$ | **56.1762** | 0.0026 | 0.1109 | 0.0372 | 0.0036 | 0.1542 |
| $^1T_2$ | **56.2726** | 0.0097 | 0.4139 | 0.1407 | 0.0127 | 0.5771 |
| $^1T_2$ | **56.3719** | 0.0008 | 0.0362 | 0.0122 | 0.0012 | 0.0503 |
| $^1T_2$ | **56.6016** | 0.0002 | 0.0066 | 0.0028 | 0.0032 | 0.0128 |
| $^1A_1$ | **56.6823** | 0.0143 | 0.5429 | 0.1944 | 0.0266 | 0.7781 |
| $^1A_1$ | **56.9149** | 0.0004 | 0.0137 | 0.0059 | 0.0046 | 0.0245 |
| $^1A_1$ | **57.0620** | 0.0002 | 0.0058 | 0.0025 | 0.0032 | 0.0117 |

up entirely of triplet states, while the higher-lying $B_2$ only of singlet states. This is easily understood in view of the strong localization of both positive charges in the same small region of space, producing singlet-triplet splitting values of the order of few eV. States with a similar $2h$ composition (see Table II) but with the two holes localized either on distinct fluorine atoms or on the same fluorine atoms, group A and groups $B_1/B_2$, respectively, are separated in energy by about 10 eV due to the larger hole-hole repulsion in the latter case. The next group of states (labeled C) are characterized as having the first hole in the outer $(2p)$ shell of one fluorine atom and the second in the inner $(2s)$ shell of a different fluorine atom. The energy gap between the lowest-lying states of group C and the highest-lying states of $B_2$ is $\sim 4$ eV. These two-site states, again characterized by the dominance of the $F_1^{-1}F_2^{-1}$ population, are followed by their one-site counterparts $D_1$ and $D_2$. Due to the presence of the inner valence hole the singlet-triplet splitting is here very large and therefore the two D subgroups are widely separated in energy by about 10 eV. Again the triplets $(D_1)$ are lying lower in energy than the singlets $(D_2)$. Group E comprises doubly ionized states of the fluorine $(2s)$ inner shell with the lowest-lying states clearly separated from the highest-lying states of group $D_2$ by almost 4 eV. Here again the two holes are localized on different atoms. The remaining group of states, F, comprises essentially singlet states with two holes in the $2s$ shell of the same fluorine atom, lying in the energy range around 100 eV. Because of the strong correlation effects in this energy range, this group spreads over many

TABLE IV. Average two-hole population and variance in percent of the total $2h$ pole strength of the eight groups of dicationic states of $SiF_4$ as well as the average $s^{-2}$, $s^{-1}p^{-1}$, and $p^{-2}$ contribution (in percent) to the main component, $F^{-2}$ or $F_1^{-1}F_2^{-1}$, respectively. The energy ranges of the groups do not overlap. The labeling of the peaks refer to the figures. The underlined numbers represent the largest und hence most relevant numbers.

| Peak | $Si^{-2}$ | $F^{-2}$ | | | $Si^{-1}F^{-1}$ | $F_1^{-1}F_2^{-1}$ | | |
|---|---|---|---|---|---|---|---|---|
| | | $s^{-2}$ | $s^{-1}p^{-1}$ | $p^{-2}$ | | $s_1^{-1}s_2^{-1}$ | $s_1^{-1}p_2^{-1}$ | $p_1^{-1}p_2^{-1}$ |
| A | 0.483 ± 0.518 | | 0.657 ± 0.830 | | 12.940 ± 6.051 | | 85.921 ± 7.037 | |
| | | | | | | 0.070 | 2.828 | 93.100 |
| $B_1$ | 0.542 ± 0.267 | | 82.166 ± 5.418 | | 15.126 ± 4.193 | | 2.166 ± 1.082 | |
| | | 0.000 | 2.885 | 97.113 | | | | |
| $B_2$ | 0.9503 ± 0.584 | | 76.395 ± 12.491 | | 17.459 ± 5.894 | | 5.195 ± 8.226 | |
| | | 1.663 | 2.729 | 95.583 | | | | |
| C | 0.661 ± 0.760 | | 1.171 ± 2.325 | | 14.530 ± 4.530 | | 83.6382 ± 5.978 | |
| | | | | | | 4.470 | 85.531 | 10.048 |
| $D_1$ | 0.446 ± 0.268 | | 73.986 ± 11.311 | | 16.827 ± 4.132 | | 8.741 ± 9.661 | |
| | | 0.108 | 89.741 | 10.062 | | | | |
| $D_2$ | 0.807 ± 0.633 | | 80.093 ± 7.268 | | 12.510 ± 2.100 | | 6.590 ± 5.575 | |
| | | 4.849 | 93.055 | 2.079 | | | | |
| E | 0.748 ± 0.310 | | 1.610 ± 1.513 | | 15.689 ± 2.383 | | 81.953 ± 2.9182 | |
| | | | | | | 86.077 | 4.550 | 9.342 |
| F | 0.863 ± 0.460 | | 51.221 ± 22.591 | | 14.398 ± 3.172 | | 33.517 ± 23.257 | |
| | | 83.830 | 11.452 | 4.714 | | | | |

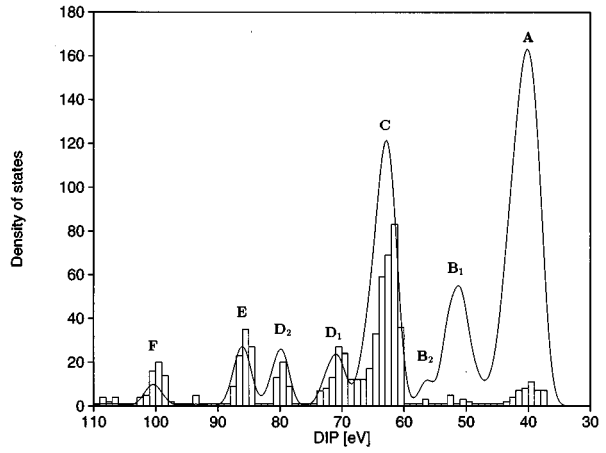


FIG. 1. The bar graph shows the density of states for the dicationic states of $SiF_4$. The curve shows the Gaussian convolution [full width at half maximum (FWHM) 2.7 eV] of the total $2h$ pole strengths (the $y$ axis in arbitrary units is scaled accordingly).

states with only very few states having a $2h$ pole strength larger than 0.1.

As Tables III and IV show, the $Si^{-2}$ and the $Si^{-1}F^{-1}$ character of the states is systematically a very small fraction of the total $2h$ pole strength. The $Si^{-1}F^{-1}$ population is typically one order of magnitude smaller than the dominating (fluorine) population, and the $Si^{-2}$ contribution about two orders of magnitude smaller. These population terms involving silicon are smaller at the low-energy end of each group of states, where the outermost purely fluorine electrons are involved, and tend to increase towards the high-energy end of each group, where the more bonding electrons are involved. It is very important to note one particular consequence of the character of the dicationic states: while for any state the fluorine one-site hole density is either dominating or, compared to the dominating term, negligibly small, the silicon one-site character is of the same relative order of magnitude for all states and spread uniformly throughout the spectrum. We shall discuss in the next section how this fact suffices to give full account of the observed Auger spectra.

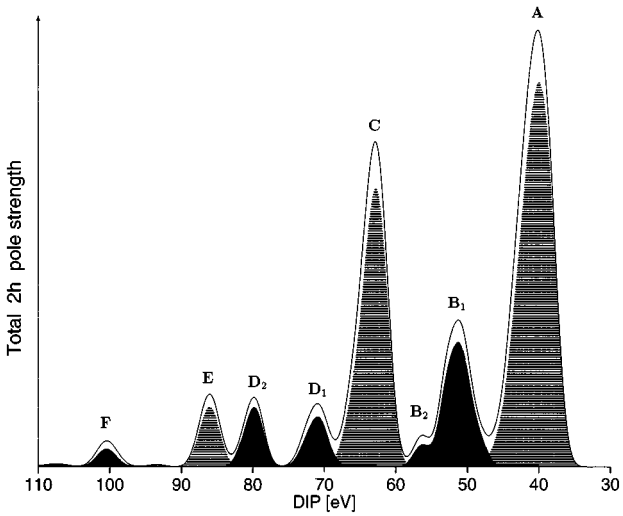


FIG. 2. The full curve represents the Gaussian convolution (FWHM 2.7 eV) of the total $2h$ pole strengths, the gray area visualizes the $F_1^{-1}F_2^{-1}$ component and the black area reflects the $F^{-2}$ component.

The results presented above thus show unquestionably that two valence electron vacancies created in a $SiF_4$ molecule have a very strong tendency to localize at the fluorine atoms, either on the same or two different ones. This is at least true for all the states that have a significant $2h$ character and thus carry Auger intensity. As we have seen, the energy distribution of these states is straightforwardly dictated by their one-site or two-site character and the atomic shells of fluorine involved. We whould like to emphasize that these conclusions are not the result of a particular interpretation of the theoretical data or just a convenient picture or discussion framework, nor can they possibly be considered an artifact of the methods we use. They derive from the straightforward analysis of the correlated wave functions of the dicationic states and summarize a genuine physical phenomenon which, as we shall discuss, leaves unmistakable fingerprints on the experimental observations. It is possible to obtain a simplified but plausible picture of the double hole localization. When two different Si–F bonds are ionized, the two holes drift towards the fluorine atoms because these are electron rich and this minimizes hole-hole repulsion. In the double ionization of the same Si–F bond, it should be expected that hole repulsion tends to separate the two positive charges, one on Si and one on F. However, the ground-state population analysis shows that the electron density around the silicon site is small and, of course, distributed over the four bonds. The full localization of even only one hole at the silicon is therefore energetically highly unfavorable and, consequently, the corresponding hole-population terms are systematically small compared to the $F^{-2}$ terms.

## V. AUGER SPECTRA

Although Auger transition probabilities are difficult quantities to compute accurately (all the more so for large polyatomics where the number of relevant final dicationic states is enormous), we can use qualitative arguments, which follow straightforwardly from the results discussed in Sec. IV, to estimate the Auger intensity distribution in the spectra based on the two-hole population analysis [17–19]. We shall thus not attempt to compute accurate intensities of individual transitions, but rather to use the results of the two-hole population analysis to achieve an unambiguous interpretation of the observed Auger bands, each consisting out of numerous states. These arguments appear particularly appropriate for $SiF_4$ because of the clear-cut localized character of the dicationic states discussed above. The Auger decay is an essentially intra-atomic process that, therefore, in a polyatomic system, can roughly be thought of as a probe of the magnitude of the two-hole density in the final dicationic states at the atomic site where the primary, decaying, core hole is created. It is clear that only states that have a significant relative component of the two-hole density located at a given atom can have an appreciable rate of decay from the corresponding core hole. We can therefore expect to observe a qualitative correspondence between the energy distribution of a given $X^{-2}$ component of the pole strength and the re-

gions of strongest intensity in the Auger spectrum originating from core ionization of atom $X$. This correspondence has indeed been shown to hold with remarkable precision [17–19], especially when, as is most often the case, the density of states is high enough for many states to contribute to each resolved Auger band.

The results of the two-hole density analysis discussed in the previous section and the above arguments lead to a straightforward prediction of the appearance of the fluorine and silicon Auger spectra in $SiF_4$. In the fluorine spectrum, the contribution of each group of states reduces to a binary yes or no choice: since all states are either fully one-site or fully two-site, they either appear in the spectrum (one-site states) or have vanishing intensity (two-site states). In other words, the states in groups B, D, and F make up the spectrum, while those in groups A, C, and E should be essentially dark. The spectrum should have a distinct atomiclike (neon like) appearance, with three separate regions of $2p^{-2}$, $2s^{-1}2p^{-1}$, and $2s^{-2}$ character, respectively. The large singlet-triplet gap separating the $D_1$ and $D_2$ components should be visible in the spectrum. This correspondence between the $F^{-2}$ population distribution, convoluted with a Gaussian envelope where each state is assigned a width of 2.0 eV, and the experimental fluorine $KLL$ spectrum of $SiF_4$ is clearly displayed in Fig. 3. As can be seen, the agreement in the overall profile and also in the individual band shapes is remarkable, leaving no doubt about the interpretation. The groups of states dominated by the $F_1^{-1}F_2^{-1}$ character do not appear. There is one intense, clearly composite, band at $\sim 50$ eV, broadened on the high-energy side and accompanied by a small peak. The theoretical spectrum drawn at the chosen resolution evidences these features accurately. This part of the spectrum corresponds to the distribution of $p^{-2}$-like states of groups $B_1$ and $B_2$ (see Table IV and Fig. 2). The two weaker bands corresponding to the $D_1$ and $D_2$ ($s^{-1}p^{-1}$) appear at $\sim 70$ and $\sim 80$ eV, respectively. The relative intensity of these peaks is in evident deviation from the experiment, but this is easily explained by the much smaller expected transition rate of the triplet states (group $D_1$), which has not been accounted for. The experimental spectrum shows an evident band between 60 and 70 eV, where only dark $F_1^{-1}F_2^{-1}$ states are computed. This is fully consistent with the attribution of this feature to shakeup and shakeoff satellites that do not belong to the normal Auger spectrum [28]. It should be noted that these satellites can in principle be eliminated from the experimental spectrum by measuring the Auger electrons in coincidence with the primary core electron. Finally the weak and broad peak of $s^{-2}$ origin (states of group F) appears at about 100 eV. The relative position of the high-energy peaks is somewhat underestimated in the calculations due to the strong relaxation effects [5], which are not completely accounted for.

The interpretation of the fluorine Auger spectrum in the light of the two-hole density analysis clarifies some relevant and general questions. Its simple atomiclike appearance emerges as the result of the pronounced localization of the two holes taking place in the dense manifold of final states. Because of the intra-atomic nature of the Auger process, this phenomenon enforces *extremely strict selection rules* on the decay transition rates, whereby more than half of the available dicationic states, comprising all the ones of $F_1^{-1}F_2^{-1}$ character, is not populated at all. Indeed, by simple counting arguments, about 3/5 of the states are forbidden. This fact deprives the fluorine spectrum of all the relevant information about the molecular environment, reducing it to an indistinct *self-image* of the fluorine atom itself, almost indistiguishable from, say, the fluorine spectrum of hydrogen fluoride. It is interesting to remark, for example, that among the totally dark states we find the lowest-lying ones, belonging to group A. This readily explains in very simple terms the fact that the onset of the spectrum is found to lie about 11 eV above the double-ionization threshold of $SiF_4$, which may be at first sight rather puzzling if one is guided only by the superficial and misleading observation that the lowest dicationic states must obviously derive from ionization of purely fluorine electrons. Its seems evident that the analogous feature characterizing the fluorine spectrum of $CF_4$ [29] can easily be understood in the light of our results [30].

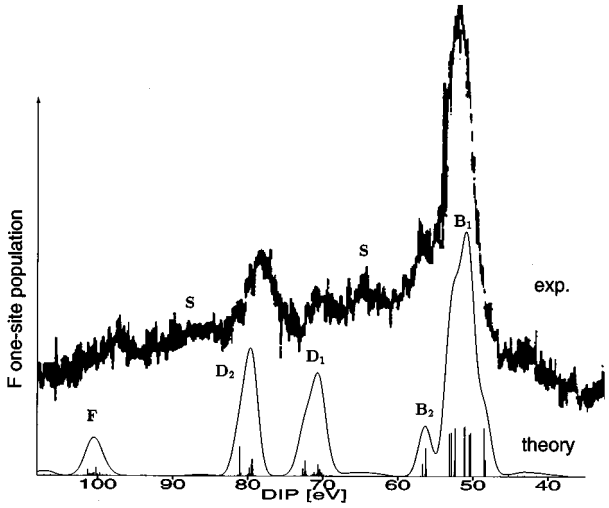


FIG. 3. Experimental (upper) and theoretical (lower) F Auger spectrum of $SiF_4$. The theoretical spectrum is obtained by Gaussian convolution (FWHM 2.0 eV) of the $F^{-2}$ two-hole populations resulting from ADC(2) calculations. Peaks indicated by s are satellites not belonging to the normal Auger spectrum [23].

By following the same lines of analysis, the apparent complexity of the silicon $LMM$ spectrum of $SiF_4$ is of immediate interpretation. The Auger process is here probing the two-hole density at the silicon site in a situation where, as we have seen, the $Si^{-2}$ population, of both $s$ and $p$ character, is small but *very uniformly distributed* over the entire spectrum of doubly ionized states. This extreme physical situation obviously prevents the occurrence of any *a priori* strong selection rule similar to those found in the fluorine spectrum and we are led to conclude that it all eight groups of states should be visible in the Si spectrum, each of the most widely spaced groups producing one separate band. The Gaussian convoluted distribution of the $Si^{-2}$ population is compared to the experimental spectrum in Fig. 4, showing a striking agreement for all the band shapes, which confirms in full our qualitative prediction. The two bands in the theoretical spectrum corresponding to the groups $B_1$ and $B_2$ are clearly not resolved in the experiment, due probably to state-specific broadening effects that we of course neglect completely. De-

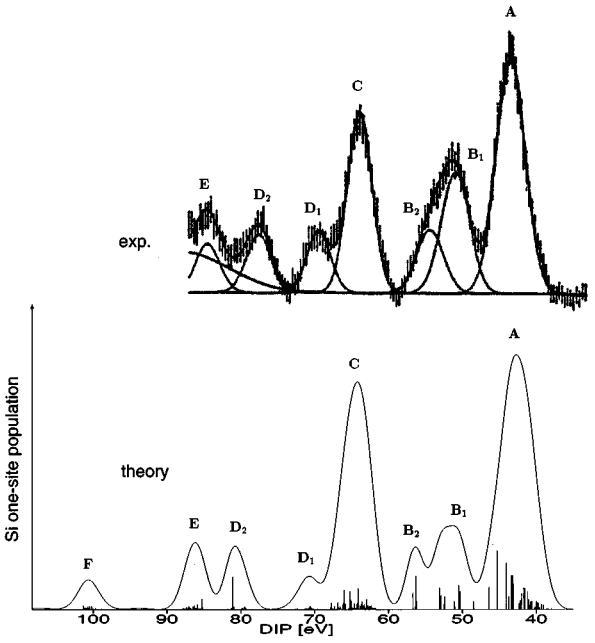


FIG. 4. Experimental (upper) and theoretical (lower) Si 2*p* Auger spectrum of $SiF_4$. The theoretical spectrum is obtained by Gaussian convolution (FWHM 2.7 eV) of the $Si^{-2}$ two-hole populations resulting from ADC(2) calculations. The underlying fit in the experimental curve was done by the experimentalists [2].

spite this, even most relative intensities of the bands are reproduced within acceptable error bounds in the computed spectrum, confirming that the distribution of one-site spectroscopic factors is what statistically dominates band formation in dense spectra [19]. This is particularly evident here since the $Si^{-2}$ terms are very small and one could expect that many effects affecting in different ways the intensity and broadening of different Auger transitions play a comparatively large role. These include, for example, decaying state satellites and nuclear dynamics effects. Our results show that, at the resolution of the compared experiment, these effects are essentially uniform throughout the spectrum and largely averaged out by the high density of states. It is illuminating to note, in this respect, the evident similarity between the (experimental or theoretical) silicon spectrum and the convolution of total $2h$ pole strengths displayed in Fig. 1. The assignment of the bands coincides essentially with the two-hole population analysis of the groups of states discussed earlier and we shall not repeat it here. Note that the highest-energy band, due to the $F^{-2}$ inner-shell ionization at about 100 eV, is computed to be very weak and broad, and lies outside the range of the experimental spectrum. It is likely that strong correlation effects beyond those accounted for in our calculations make this band even broader and hardly detectable.

The conceptual differences between the results of Auger decay from the fluorine and silicon core holes stand out very evidently from our analysis. While the fluorine spectrum is strictly atomic in appearance, bearing no trace of the chemical environment, exactly the opposite is true for the silicon spectrum. Here all the atomic information is lost and the spectrum reflects in every detail the full set of dicationic states, whose energy distribution is exclusively determined by the surrounding molecular environment where the electron vacancies are produced. This characteristic of Auger spectra has been defined *foreign imaging* [5] and is fully confirmed by the present work. The Si spectrum of $SiF_4$ represents a prototype example of this phenomenon, where the lack of selection rules is practically complete. This feature may at first sight seem to contradict the intra-atomic character of the Auger decay, but it should be emphasized that it is, on the contrary, a direct consequence of it. The silicon atom undergoes a pronounced electron loss upon binding four fluorine atoms, and there is hardly any trace of the electronic structure of $Si^{2+}$ present in the molecular dication. Thus, it is plainly impossible to relate the Si spectrum of $SiF_4$ to that of the isolated atom. Because of the intra-atomic dominance of Auger decay rates, it is precisely this absence of a discernible silicon dication to be reflected by the loss of atomic information in the molecular spectrum.

## VI. SUMMARY AND CONCLUSIONS

In the present work we have performed *ab initio* Green's-function calculations beyond second-order perturbation theory on the whole double-ionization spectrum of silicon tetrafluoride, comprising many thousands of states, in order to study its Auger spectra and, in particular, to arrive at the definitive interpretation of the puzzling silicon $LMM$ spectrum. The calculation at this level of theory, which is the least required to obtain a conclusive noncontroversial picture of the phenomena involved, have been rendered feasible by the use of a block-Lanczos technique to achieve rapid convergence on the envelope of the dense two-hole pole strength distribution.

A population analysis of the correlated two-hole density thus obtained has shown that in all the dicationic states of $SiF_4$ the two-electron vacancies are strongly localized at the fluorine atoms, either each on a different atom or both on the same. This two-site or one-site hole localization and the outer or inner valence character of the ionized electrons dictates, via hole-hole repulsion, the energy distribution of the states, which come in dense and well-separated groups. The $Si^{-2}$ component of the two-hole density is orders of magnitude smaller and uniformly distributed over all groups.

Seen in the light of the intra-atomic nature of Auger decay, this provides the key to understanding the character and appearance of the Auger spectra of $SiF_4$. Very strict selection rules are imposed on the fluorine spectrum, where only one-site $F^{-2}$ states are active, and none on the silicon spectrum, where essentially all the dicationic states are observed. Theoretical spectra obtained by convolution of the appropriate one-site pole strengths are found to be in close agreement with experiment.

The most remarkable aspect of the Auger spectroscopy of $SiF_4$ and similar systems is that all the information concerning the molecular system is filtered out of the ligand (fluorine) spectrum, which is strictly atomiclike, and entirely transferred to the central atom (silicon) spectrum. The latter, because of hole localization at the ligands, loses all atomic information and yields instead a complete and detailed image of the surrounding molecular environment where the electron vacancies are located. This scenario was already proposed on the basis of preliminary model calculations and named *for-*

*eign imaging* [5]. The present extensive calculation conclusively confirms its existence and general relevance. $SiF_4$ is an extreme example of this situation, but a continuous wide range of very interesting ''weaker'' cases exist. A foreign-imaging spectrum is determined by the systematically very small magnitude of the relevant one-site pole strength, which enables the surrounding environment to leave its fingerprint on the spectrum. Two-hole localization and the uniformity of the one-site density distribution may, however, be less pronounced and patterned than in $SiF_4$, giving rise to more structured and complex spectra. The carbon spectrum of the less ionic $CF_4$ molecule is one appropriate example of this [30]. In all these cases, it is expected that the concepts and guidelines illustrated in the present work may serve as a useful toolbox for analysis.

## ACKNOWLEDGMENTS

We would like to thank H.-D. Meyer for providing us with the block-Lanczos computer code and D. Schulte for technical help. Financial support by the Deutsche Forschungsgemeinschaft is gratefully acknowledged. The authors also wish to thank the ''Vigoni'' programme between CRUI, Italy, and DAAD, Germany, for financial support.

[1] R. R. Rye and J. E. Houston, J. Chem. Phys. **78**, 4321 (1983).
[2] S. Aksela, K. H. Tan, H. Aksela, and G. M. Bancroft, Phys. Rev. A **33**, 258 (1986).
[3] T. A. Ferrett, M. N Piancastelli, D. W. Lindle, P. A. Heimann, and D. A. Shirley, Phys. Rev. A **38**, 701 (1988).
[4] G. G. B. de Souza, P. Morin, and I. Nenner, J. Chem. Phys. **90**, 7071 (1989).
[5] F. Tarantelli and L. S. Cederbaum, Phys. Rev. Lett. **71**, 649 (1993).
[6] F. P. Larkins, J. McColl, and E. Z. Chelkowska, J. Electron. Spectrosc. Relat. Phenom. **67**, 275 (1994).
[7] T. D. Thomas and P. Weightman, Chem. Phys. Lett. **81**, 325 (1981).
[8] P. Weightman, T. D. Thomas and D. R. Jennison, J. Chem. Phys. **78**, 1652 (1982).
[9] F. Tarantelli, A. Sgamellotti, and L. S. Cederbaum, J. Chem. Phys. **94**, 523 (1991).
[10] R. Arneberg, J. Müller, and R. Manne, Chem. Phys. **64**, 249 (1982).
[11] O. M. Kvalheim, Chem. Phys. Lett. **86**, 159 (1982).
[12] O. M. Kvalheim, Chem. Phys. Lett. **98**, 457 (1983).
[13] J. Schirmer and B. Barth, Z. Phys. A **317**, 267 (1984).
[14] A. Tarantelli and L. S. Cederbaum, Phys. Rev. A **39**, 1639 (1989).
[15] E. M. -L. Ohrendorf, H. Köppel, L. S. Cederbaum, F. Tarantelli, and A. Sgamellotti, J. Chem. Phys. **91**, 1734 (1989).
[16] E. M. -L. Ohrendorf, F. Tarantelli, and L. S. Cederbaum, J. Chem. Phys. **92**, 2984 (1990).
[17] D. Minelli, F. Tarantelli, A. Sgamellotti, and L. S. Cederbaum, J. Chem. Phys. **99**, 6688 (1993).
[18] D. Minelli, F. Tarantelli, A. Sgamellotti, and L. S. Cederbaum, J. Electron. Spectrosc. Relat. Phenom. **74**, 1 (1995).
[19] F. Tarantelli, A. Sgamellotti, and L. S. Cederbaum, in *Applied Many-Body Methods in Spectroscopy and Electronic Structure*, edited by D. Mukherjee (Plenum, New York, 1992).
[20] F. P. Larkins, J. Electron. Spectrosc. Relat. Phenom. **51**, 115 (1990).
[21] H. Ågren, A. Cesar, and C. M. Liegener, Adv. Quant. Chem. **23**, 1 (1992).
[22] T. H. Dunning, J. Chem. Phys. **55**, 716 (1971).
[23] A. D. McLean and G. S. Chandler, J. Chem. Phys. **72**, 5639 (1980).
[24] A. Ahlrichs and P. R. Taylor, J. Chem. Phys. **78**, 315 (1981).
[25] L. E. Sutton, *Tables of Interatomic Distances and Configurations in Molecules and Ions* (The Chemical Society, London, 1958).
[26] H.-D. Meyer and S. Pal, J. Chem. Phys. **91**, 6195 (1989).
[27] F. O. Gottfried, F. Tarantelli, and L. S. Cederbaum (unpublished).
[28] K. Zähringer, H.-D. Meyer, L. S. Cederbaum, F. Tarantelli, and A. Sgamellotti, Chem. Phys. Lett. **206**, 247 (1993).
[29] W. J. Griffiths, S. Svensson, A. Naves de Brito, N. Correia, C. J. Reid, M. L Langford, F. M. Harris, C. M. Liegener, and H. Ågren, Chem. Phys. **173**, 109 (1993).
[30] F. O. Gottfried, F. Tarantelli, and L. S. Cederbaum (unpublished).